High Frequency (6 Hz) PKPab precursors and their sensitivity to deep Earth heterogeneity

Christoph Sens-Schönfelder[1], Klaus Dieter Bataille[2], and Marcelo Bianchi[3]

[1]GeoForschungsZentrum Potsdam
[2]Universidad de Concepcion
[3]Universidade de Sao Paulo

November 24, 2022

Abstract

We present observations on a new precursory phase of seismic waves scattered in the deep Earth. This phase arrives prior to the PKPab wave at epicentral distances larger than 155º, and we call it PKPab precursor. We show that the presence of the PKPab precursor is a necessary consequence of scattering in D'', which is the commonly accepted cause of the PKPdf precursor at distances smaller than 145º. PKPdf waves that propagate through the inner core should arrive before the PKPab precursor but those, are strongly attenuated in the inner core at frequencies between 4 Hz and 8 Hz used here, making the PKPab precursor the earliest teleseismic signal at distances larger than 155º. Calculated PKPab precursor sensitivity kernel shows that this phase is mostly sensitive to scattering along the closest PKPbc path between source and receiver. It can thus help to constrain the lateral distribution of heterogeneity along D".

High Frequency (6 Hz) PKPab precursors and their sensitivity to deep Earth heterogeneity

C. Sens-Schönfelder[1], K. Bataille[2,1], M. Bianchi[3]

[1]GFZ German Research Centre for Geosciences, Telegrafenberg, 14473 Potsdam, Germany
[2]Earth Sciences Department, University of Concepcin, Chile
[3]Instituto de Astronomia, Geofsica e Cincias Atmosfricas, Universidade de So Paulo, Brazil

Key Points:

- PKP precursor observed at distance beyond 155 deg
- D" scattering of teleseismic waves at 6Hz
- radiative transfer simulation used to locate regions of heterogeneity

Corresponding author: Christoph Sens-Schnfelder, `sens-schoenfelder@gfz-potsdam.de`

Abstract

We present observations on a new precursory phase of seismic waves scattered in the deep Earth. This phase arrives prior to the $PKPab$ wave at epicentral distances larger than 155°, and we call it $PKPab$ precursor. We show that the presence of the $PKPab$ precursor is a necessary consequence of scattering in D", which is the commonly accepted cause of the $PKPdf$ precursor at distances smaller than 145°. $PKPdf$ waves that propagate through the inner core should arrive before the $PKPab$ precursor but those, are strongly attenuated in the inner core at frequencies between 4 Hz and 8 Hz used here, making the $PKPab$ precursor the earliest teleseismic signal at distances larger than 155°. Calculated $PKPab$ precursor sensitivity kernel shows that this phase is mostly sensitive to scattering along the closest $PKPbc$ path between source and receiver. It can thus help to constrain the lateral distribution of heterogeneity along D".

Plain Language Summary

A new discovered seismic signal recorded far away from earthquakes, by stations on the other side of Earth, will help to study the properties of the core-mantle boundary. We use high frequencies at which seismic waves do not propagate through the Earth's inner core but are instead propagated around it by deflection at heterogeneity located along the core-mantle boundary.

1 Introduction

1.1 Deep Earth structure

The boundary between the core and mantle of the Earth is one fascinating region in the deep Earth (Tackley, 2012). Here the solid mantle that consists of silicic minerals is in contact with a liquid mostly consisting of molten iron. The density contrast between the core ($\rho = 9,900 kg/m^3$) and the mantle ($\rho = 5,800 kg/m^3$) is about twice as high as the difference between air and the crust at the Earth's surface, but at the core-mantle boundary (CMB) the liquid is heavier, while gravitational acceleration is similar to the Earth surface conditions. At this odd interface, lightweight components of the core material, potentially generated by solidification of heavier components, accumulate from below (Buffett et al., 2000; O'Rourke & Stevenson, 2016), as well as heavy components of the mantle, accumulate from above. These processes caused significant heterogeneity in the D"-layer at the base of the mantle.

The core-mantle boundary is of significant interest in the dynamics of our planet. CMB plays a vital role in two major geodynamic processes as it interfaces the outer core that generates Earth's magnetic field and the mantle that hosts plate tectonics. Processes and structure of the CMB control plate tectonics engine fueled by the heat from the core. The geodynamo depends on continuous convection in the core that is, in turn, also controlled by heat transfer through the boundary (Olson, 2016; Labrosse, 2014). The CMB is believed to be the source region of magmatic plumes that led to episodes of gigantic volcanic activity at the surface, accompanied by mass extinction events (Courtillot & Renne, 2003).

The lowermost 200 km of the mantle form a high complexity zone, the so-called D" layer. Images of the D" have been presented by Global seismic tomography studies (Kustowski et al., 2008; Ritsema et al., 2011) while its structure is determined generally using top and bottom reflections as well as transmitted and diffracted waves (Wang & Wen, 2004; Sun et al., 2013; Frost & Rost, 2014; Shen et al., 2016; Euler & Wysession, 2017; Hansen et al., 2020) observations. A review of seismic investigations of the lower mantle can be found in Lay and Garnero (2011). D" hosts large low shear velocity provinces

(LLSVP) and ultra low-velocity zones (ULVZ) as reviewed in Yu and Garnero (2018) and McNamara (2019).

Whereas the ULVZ are local features with a lateral extent of 100s of kilometers, the two LLSVP are global features beneath Africa and the Pacific. These regions are associated with large scale material uplift in the global mantle convection. There is no real consensus about the nature of the LLSVP, and potential explanations range from purely thermal anomalies to chemically distinct regions in the lower mantle. From their locations, the LLSVPs are believed to be the hottest regions in the mantle since they match the base of global upwelling. This idea is also confirmed by a large number of hotspots and mantle plumes above them.

Hypotheses for the origin of the LLSVPs include primordial thermochemical piles of high-density material that accumulated early on in Earth's history and formed a basal mélange (Tackley, 2012). Other Hypotheses propose the accumulation of chemical heterogeneity over long geologic timescales through subducted oceanic crust (Li et al., 2014). The presence of post-perovskite (Koelemeijer et al., 2016) best explains the seismic signature of the LLSVP with a reduced shear wave velocity and a normal compressional wave velocity. Estimates of the vertical extent of the LLSVP above the CMB reach up to several 100s of kilometers (McNamara, 2019). The structure at the top of the LLSVP depends on the plumes that rise from the LLSVP. While some geodynamic models predict plumes rising predominantly from the edges of LLSVPs, others predict that smaller plumes may rise from the top of the entire LLSVP area. In fact, the LLSVPs could consist of many thin plumes that focus on large-scale upwelling areas and appear as continuous low velocity features only due to tomographic filtering (Schuberth et al., 2009).

In summary, seismological observations and geodynamic models demonstrated that the lower mantle is a region that might be characterized by chemical heterogeneity but is undoubtedly subject to thermal heterogeneity. Due to viscosity dependence of temperature, the length scale of the thermal heterogeneity can be significantly smaller than what is expected from thermal diffusion, e.g., by the formation of narrow plumes.

1.2 Wave scattering in the deep Earth

From geological structures at the surface and the investigation of high-frequency wave scattering in the Earth's crust, we know that geological materials differ not only in their large scale average elastic properties like wave velocity but also, in their small scale internal structure at a length scale below the resolution of seismic imaging (Sato et al., 2012). The statistical properties of these elastic parameter fluctuations are characteristic of the geologic material and can be observed due to the signatures they leave in seismograms. When seismic waves propagate through a heterogeneous medium, the waves are scattered and frequently change direction such that interference generates a complex wavefield (Sato et al., 2012). Scattering in the Earth's crust generates coda waves that follow the arrival of ballistic phases from local or teleseismic earthquakes (Obara & Sato, 1995; Sens-Schönfelder et al., 2009; Gaebler et al., 2015). The envelope of such complex wavefields can be used to investigate the statistical properties of the heterogeneity. The interplay between the length scale of the heterogeneity, wavelength, and intrinsic attenuation of seismic waves causes scattered waves to be best observed at frequencies above 1 Hz. Investigation Earth with scattered waves is different from ballistic waves. Scattered waves do not propagate along deterministic paths predicted by ray theory, but reach the receiver on complicated trajectories that can only be described in a probabilistic sense (Pacheco & Snieder, 2005).

Since the wave velocity at the core is lower than at the mantle, scattering in the deep Earth can cause seismic energy to arrive both at the coda of a ballistic phase and prior to a ballistic phase as a precursor.

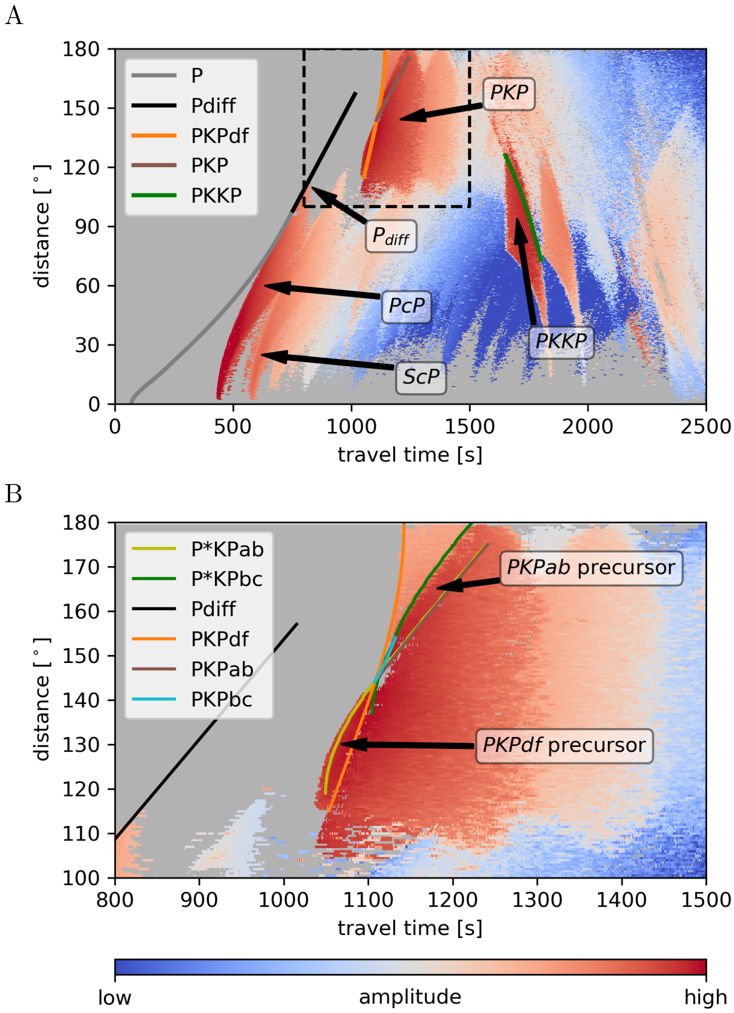

Figure 1. Increase of seismic intensity due to scattering in a 50 km thick layer above the CMB. Simulations used a 600 km deep P-wave source in the velocity and attenuation model ak135-f (Kennett et al., 1995; Montagner & Kennett, 1996). (A) Arrival times of seismic phases and relevant regions of the time-distance domain that have been investigated for scattering in the deep Earth are indicated. (B) zoom into the time-distance window of PKP waves (dashed box, panel A). Theoretical arrival times for waves scattered at the CMB are indicated and labeled with '*' indicating the scattering event. The frequently discussed $PKPdf$ precursor and the $PKPab$ precursor discussed below are labeled.

Figure 1 shows the increase of scattered intensity due to a 50 km thick scattering layer above the CMB simulated with differential radiative transfer simulations as detailed in the supporting information Text S1 which contains additional references to Takeuchi (2016) and Trabant et al. (2012). It shows a number of time-distance windows of the global wave field that have been investigated for waves scattered in the deep Earth. ScP and PcP top side reflections at the CMB can show precursors that originate by reflections above the CMB as well as coda waves from reverberations in the heterogeneous layer or off great-circle reflections (Wu et al., 2014; Gassner et al., 2015; Shen et al., 2016). Short distance $PKKP$ precursors (A. Chang & Cleary, 1978; A. C. Chang & Cleary, 1981; P. S. Earle & Shearer, 1997) also originate from off great-circle bottom side reflections at the CMB (c.f. Figure 1A). PKP precursors probe the D" layer in near-vertical transmission. Scattering of the $PKPab$ branch can divert waves in the distance range up to 145° which would not be accessible to $PKPab$, otherwise (Haddon & Cleary, 1974; Hedlin et al., 1997). These waves form $PKPdf$ precursors that arrive before the $PKPdf$ phase that travels through the inner core ($PKIKP$) and is the earliest phase in the core shadow. This situation provides exceptional conditions for the observation of $PKPdf$ precursors (c.f. Fig. 1B). Opportunities to probe the lower mantle by transmission in a near-horizontal direction is provided by P_{diff} coda (c.f. Fig. 1). While diffraction along the core-mantle boundary vanishes with increasing frequency, at short period P_{diff} coda waves in the core shadow zone, have been interpreted as a sign of scattering along the CMB (Bataille & Lund, 1996) or, as a signature of scattering throughout the mantle (P. Earle & Shearer, 2001). An overview of the travel time-distance windows in which scattered waves from the deep Earth can be observed, is given in Shearer (2007).

Understanding the origin of such faint signals arriving from the deep Earth provides a powerful tool to investigate the small scale structure of the deep mantle in terms of its statistical properties, i.e., the strength of elastic parameter fluctuations and their size distribution. It can yield valuable information about the distribution of chemical or thermal heterogeneity without the blurring effect of the tomographic filter. It also may help to constrain the depth extent and lateral distribution of features like plume clusters (McNamara, 2019), or accumulations of heterogeneous material in the basal mélange formed from subducted slabs (Tackley, 2012).

2 Observation of the $PKPab$ precursors

Additionally to the $PKPdf$ precursor at $\Delta < 145°$, Fig. 1B shows a further arrival of scattered energy at distances $\Delta > 155°$. For reasons discussed later, we term this phase $PKPab$ precursor. This phase has been discussed sporadically in the literature, and there is no consensus about its origin. Waves propagating through the inner core arrive earlier in this distance range, and it is not clear whether the scattered energy that arrives between the $PKPdf$ and $PKPab$ should be regarded as a coda of $PKPdf$ or as a precursory signal to $PKPab$. In contrast to the $PKPdf$ precursor at $\Delta < 145°$ the $PKPab$ precursor at $\Delta > 155°$ in Fig. 1 might thus be hidden in the $PKPdf$ coda depending on the relative strength of both signals.

A possibility to observe the $PKPab$ precursor unambiguously is to show its spatial coherency over an extended distance range. To avoid the effect of source-side crustal scattering, we use large deep earthquakes. Since lateral variability of D" scattering could disturb the spatial coherency when records from different areas are combined, we try to use records from compact regions. Deep sources in South America recorded by the dense Japanese HiNet seismic stations (NIED, 2019; Okada et al., 2004; Obara et al., 2005) offer a perfect source-receiver configuration to observe the desired signals.

Fig. 2 shows HiNet vertical seismogram envelopes from two events stacked in 1° distance bins. The first is a 570 km deep event with Mw 6.8 from January 1st, 2011, in Argentina that covers $151° < \Delta < 167°$ while the 592 km deep Mw 7.5 Peru event

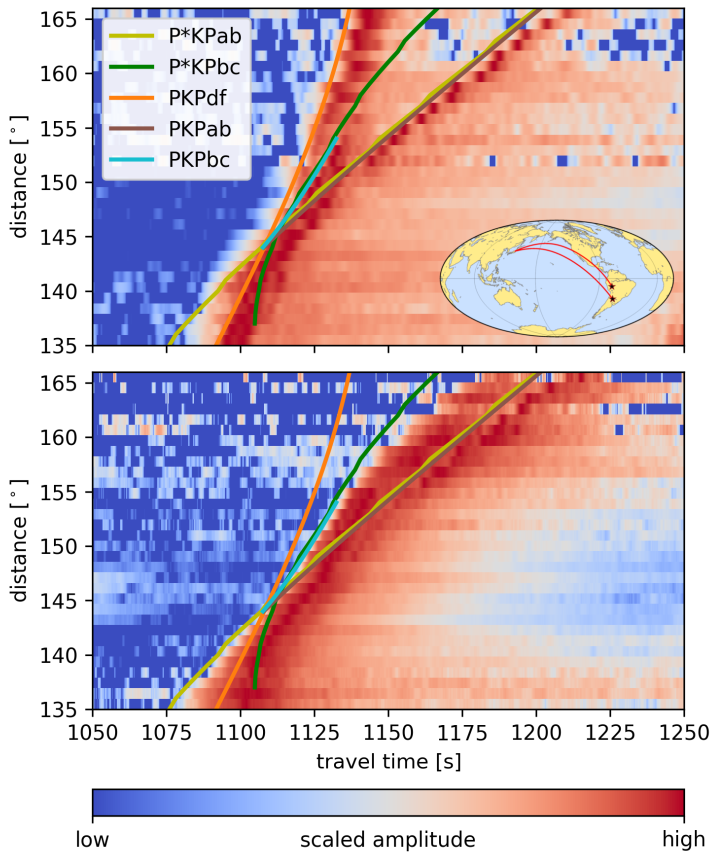

Figure 2. Composite image of stacked seismogram envelopes from Argentina and Peru deep earthquakes recorded in Japan. Arrival times of ballistic and scattered core phases are indicated. Top and bottom panels show the 0.35 - 0.7 Hz 4 - 8 Hz frequency bands, respectively. The logarithmic color scale is scaled between maximum and noise level for the individual distance bins. Inset shows the great circle between epicentres (stars) and recording stations.

from November 24th, 2015, covers $135° < \Delta < 152°$. Data processing for figure Fig. 2 is described in the supporting information Text S2. Two frequency bands are shown in Fig. 2. The low-frequency band between 0.35 Hz and 0.7 Hz shows energetic arrivals following the $PKPdf$ and $PKPab$ travel time curves and some energy arriving prior to the $PKPdf$ below 145° – the known $PKPdf$ precursor. Fig. 2B and Figures S1 and S2 (supporting information) show the same data filtered in the 4-8 Hz frequency band and differs significantly from the low-frequency panel.

Three main observations can be made: (A) Significant amount of energy travels through the entire Earth in the 4-8 Hz band. (B) The $PKPdf$ phase is strongly attenuated on the path from Peru to Japan at these high frequencies compared to the $PKPab$ phase. There is no indication of energy propagating through the inner core in the 4-8 Hz band. (C) A distinct increase of energy follows the lines of the earliest possible scattered energy arrival from the CMB as indicated by the lines labeled $P{*}KPab$ and $P{*}KPbc$ in Fig. 2. We call this phase $PKPab$ precursor.

We would like to emphasize that the presence of the $PKPab$ precursor is not due to a local effect at the source of the event (Argentina) or local disturbances within the

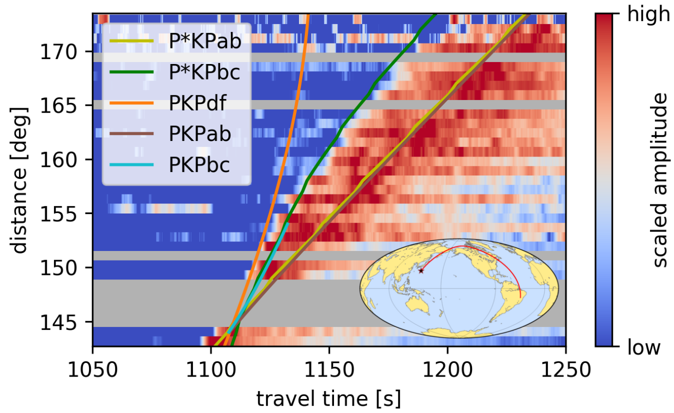

Figure 3. Stacked seismogram envelopes from the Bonin deep earthquakes recorded in Brazil. Arrival times of ballistic and scattered core phases are indicated. Gray intervals represent gaps in the distance coverage of the network. The logarithmic color scale is scaled as in Fig. 2. Inset shows the great circle between epicentre (star) and station network.

HiNet. Fig. 3 shows the stacked envelopes of the May 30th, 2015 deep Bonin Islands earthquake (Mw 7.8, depth 677 km) recorded at stations from part of the Brazillian Seismographic Network (Bianchi et al., 2018), network codes BL and BR. A clear signal of the $PKPab$ precursor following the $P*KPbc$ arrival time is observed for this wave path, too.

3 Origin of the $PKPab$ precursor

The onset of $PKPab$ precursor emerges at the c-caustic that connects the $PKPbc$ and $PKiKP$ (inner core reflection) branches with a common slowness. Thus, it seems reasonable to assume a relation of the $PKPab$ precursor to one of these two phases. Possible mechanisms could be (A) diffraction of $PKiKP$ waves along the inner core boundary (ICB) or the propagation through a heterogeneous waveguide above the ICB, or (B) deviation of $PKPbc$ waves into the shadow of the inner core by scattering in the mantle or outer core. Feasibility to differentiate between these two possibilities is provided by the slowness-distance relation of the earliest energy arrival. For mechanism (A), the energy diffracted along the ICB should arrive with constant slowness for all distances. This should be the slowness of $PKiKP$ waves at the c-caustic or a somewhat higher but constant slowness if a low-velocity layer is invoked at the ICB. Since the onset of the scattered energy is clearly curved to higher slowness for increasing distances (Fig. 2C and 3) the observations do not favor the ICB-diffraction mechanism (A).

Mechanism (B) i.e., the deviation of $PKPbc$ wave direction, would mean that part of the $PKPbc$ wave energy that travels just atop the inner core gets scattered on its path through the Earth. Depending on the depth distribution of the heterogeneity that causes the scattering, different onset times are possible. However, from the $PKPdf$ precursor at distances $\Delta < 145°$ it is known that especially the D" layer above the CMB scatters wave energy, and is thus a right candidate.

Deviating the propagation direction of $PKPab$ waves at the source (or receiver) side to create $P{*}KPab$ ($PKab{*}P$) waves explains the arrival time of the $PKPdf$ precursor energy for $\Delta < 145°$ (Fig. 2). For $\Delta > 145°$ $P*KPab$ energy arrives coincident with ballistic $PKPab$.

On the other hand, deviating the propagation direction of $PKPbc$ waves at D" can shed energy in the distance range $\Delta < 145°$ that arrives after the $PKPdf$ precursor and the $PKPdf$ wave and is thus hard to observe. For $\Delta > 155°$ the $P*KPbc$ energy arrives prior to the $PKPab$ phase. Since the earlier $PKPdf$ arrival is strongly attenuated in the high frequency, as shown in Fig. 2, the scattered $P*KPbc$ energy forms the first notable arrival.

We summarize that (A) scattering of core phases in the lower mantle is a commonly accepted process as confirmed for example by the $PKPdf$ precursor at $\Delta < 145°$ and (B) in simulations of energy propagation considering a scattering in the lower mantle predict the arrival of energy that is in qualitative agreement with the observation of the $PKPab$ precursor (compare Fig. 1 and 2, 3). These ideas strongly support the hypothesis that the observed $PKPab$ precursor at $\Delta > 155°$ is a consequence of the same process that causes the well known PKP precursor at $\Delta < 145°$.

4 Local Sensitivity of the *PKPab* Precursor to Scattering

Waves scattered in the deep Earth provide means to investigate the structure of the lower mantle at a spatial scale below the resolution limits of seismic tomography. The $PKPab$ precursor offers a new opportunity for this. Here we investigate the spatial sensitivity of this signal. We use the theory of Margerin et al. (2016) and Zhang et al. (2020) to derive an intensity sensitivity kernel, which describes the sensitivity of the seismogram envelope to a local increase of scattering strength. We simplify the treatment in three ways. (A) Wave propagation through the inner core is blocked. Since we observe that $PKPdf$ waves vanish in the 4-8 Hz frequency range (cf. Fig. 2, 3, S1), waves that propagate through the inner core cannot contribute to the scattered arrival either. Scattering within the inner core would generate $PKPdf$-coda rather than a separate phase that is disconnected from the $PKPdf$ arrival. (B) We assume that scattering leading to the $PKPab$ precursor is isotropic, which simplifies the treatment of scattering angles. Increased probability of forward scattering would reduce the probability of scattering close to either source or receiver. (C) The scattering process is restricted to a single scattering of P-waves because S-wave propagation is highly unlikely for the short travel time of the $PKPab$ precursor.

Under the assumptions made, we can calculate the volume in which scattering can contribute to the observed $PKPab$ precursor by convolution of the forward and backward P-wave intensity. These intensities can be obtained by radiative transfer simulations, as described in Text S1 for excitation at the location of the earthquake (forward simulation) and the location of the receiver (backward simulation). The sensitivity finally describes the probability of a wave packet that arrives in a particular time-distance window to have traveled from the source to a particular location in space where scattering occurred, and then continued to the receiver location.

Fig. 4A shows a cross-section through the sensitivity kernel in the great circle plane for an epicentral distance of $\Delta = 160°$ and a lapse time of 1155 s, which is within the time-distance window of the $PKPab$ precursor. It describes the influence of heterogeneity (i.e. the possibility for wave scattering) on the amplitude of the $PKPab$ precursor. Regions, where this probability is high, have a strong influence on the precursor amplitude. If this probability is low at some location, the influence is weak because it is unlikely that a wave arriving in the time-distance window was scattered there. Zero influence means that it is impossible for wave energy to arrive in the time-distance window of the $PKPab$ precursor even if it is scattered there.

High sensitivity is located along the $PKPbc$ path through the outer core and lower mantle. In this narrow volume, waves are scattered mostly in the forward direction meaning that small perturbations of the propagation direction of $PKPbc$ waves can gener-

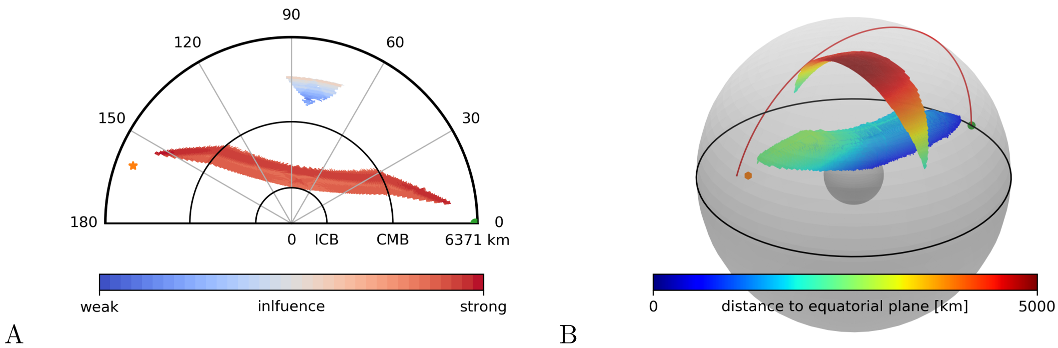

Figure 4. Volume of sensitivity for an arrival at 1155 s lapse time and epicentral distance of $\Delta = 160°$. Orange star and green circle indicate locations of source and receiver, respectively. (A) cross section in the great circle plane of source and receiver with warm colors indicating high sensitivity of the arrival to scattering. CMB and ICB are indicated. (B) 3D representation of the volume of sensitivity with color indicating distance to the equatorial plane. Two distinct regions of sensitivity exist. One is draped on the inner core along the $PKPbc$ path. Due to the high PKP amplitudes heterogeneity in this volume has a strong influence on amplitudes of the precursor. Another sickle-shaped region of sensitivity that allows for large deviations form the great circle is formed by scattering of P waves in the mantle. Heterogeneity in this region, however, has less influence on the amplitude of the $PKPab$ precursor than in the elongated region that extends through the deep Earth (c.f. Fig. 4A).

ate the $PKPab$ precursor at 1155 s at 160° distance. Due to the high amplitude of the PKP phase the influence of this region on the $PKPab$ precursor amplitude is high as indicated by the color in Fig. 4A. Another patch of sensitivity is located in the mid mantle. It indicates that scattering of P-waves in the mid mantle allows waves to travel around the slow outer core and still carry energy to a receiver in the time-distance window of the $PKPab$ precursor. However, considering the smaller amplitudes of the participating waves, there is a low probability that the scattering in this region contributes to the observed signal – resulting in a weak influence of this region on the precursor.

Since scattering allows for off great-circle path propagation, the sensitivity has a significant 3D component, as illustrated in Fig. 4B. The volume with the strong influence on the $PKPab$ precursor that extends through the deep Earth is draped on the inner core and shows small deviations from the great-circle plane. The region of P wave scattering in the mid mantle forms a sickle-shaped volume of sensitivity, perpendicular to the great circle plane. Energy in the $PKPab$ precursor window that were scattered in the mantle can, therefore, arrive with significant deviations from the great-circle direction.

5 Discussion

Using numerical simulations, we show that scattering in the lower mantle results in the arrival of scattered energy before the $PKPab$ at $\Delta > 155°$. This energy arrives after $PKPdf$. In the high-frequency band between 4 and 8 Hz, waves do not propagate through the inner core on the path between South America and Japan. This vanishing of the $PKPdf$ energy makes the $PKPab$ precursor the first notable arrival of the record, which can be readily observed in individual records of deep earthquakes. We speculate the $PKPab$ precursory signal is also present at lower frequencies where it is masked by the earlier $PKPdf$ arrival and its coda.

The origin of the $PKPab$ precursor has been discussed earlier. A number of articles discussed the $PKP{-}C_{diff}$ phase that should result from the diffraction of compressional waves around the inner core along the ICB. Nakanishi (1990) present observations of 2.5-3.3 Hz $PKP - C_{diff}$ waves in the distance range $152° < \Delta < 157°$. From the complex, long-lasting waveforms, their earliest arrival and the high slowness Nakanishi (1990) concluded that scattering at the base of the upper mantle around 660 km depth is more likely to generate these arrivals than ICB diffraction. Tanaka (2005) investigated $PKP{-}C_{diff}$ coda using short-period seismic arrays and found slowness ranging between 1 and $5s/°$ extending through the whole range covered by $PKPab$ and $PKPbc$ waves. Scattering at the CMB was invoked as an alternative origin of the $PKP{-}C_{diff}$ coda signal, since the slowness of waves scattered close to the c-caustic is close to that of $PKP{-}c_{diff}$ waves to be separated by the arrays. These early works are thus in agreement with our interpretation of the $PKPab$ precursor as scattered $PKPbc$ with a likely location of the scattering close to the CMB.

Adam and Romanowicz (2015) report on a scattered phase that arrives 5-20 s after the $PKPbc$ of $PKPbc_{diff}$ which they call $M-$phase. Adam and Romanowicz (2015) uses coherent stacking of 1 Hz signals within distance ranges up to 10° and concludes that the scattered M-phase originates at the ICB. Scattering at the CMB is ruled out because the M-phase appears as an isolated phase in the phase weighted stack with a slowness between $0.7 - 1.6s/°$. This slowness is to low for $PKPbc$ waves scattered at the CMB beyond 160° distance. This finding appears to contradict our interpretation. However, firstly the 1 Hz frequency range differs from our observation and the argument that Adam and Romanowicz (2015) uses to rule out the possibility of $PKPbc$ scattering close to the CMB is strongly based on the limitation of the slowness range to $1.6s/°$ maximum. This constraint is derived under the assumption of distance independent slowness even though it is not shown that the M-phase at $\Delta > 160°$ has a slowness below $1.6s/°$. The fact that the M-phase appears as an isolated phase is enforced by the phase weighted stacking and did not exclude the actual presence of an extended wave train originating from waves with a significant spread of slowness.

Thus, we think that our interpretation of the $PKPab$ precursor, as scattered $PKPbc$ waves is compatible with earlier studies. The discussed $PKP{-}C_{diff}$ phase, as well as the M-phase, may be interpreted as a signal with the same origin. Since the heterogeneity at D" is widely accepted, it should be taken into account in any interpretation of signals that might have passed through D". In fact, this is true for all investigations of the inner core. The difference in coda decay between PcP and $PKiKP$ coda at small distances should not be interpreted without considering the effect of the twofold $PKiKP$ transmissions through D" which can significantly alter the shape of the coda.

The possibility to observe the $PKPab$ precursor at $\Delta > 155°$ requires strong attenuation of the earlier arriving $PKPdf$ waves that pass through the inner core. Longitudinal variations of $PKiKP$ vs. $PKPdf$ travel time and amplitude differences indicate hemispherical asymmetry of inner core attenuation (Monnereau et al., 2010). Moreover, this will likely influence the observability of the $PKPab$ precursor. The $PKPab$ precursor in locations where it can be observed can increase the lateral resolution of PKP CMB based studies. Combined with $PKPdf$, it allows using earthquakes from a much wider distance range.

As indicated by the elongated shape of the sensitivity kernel in Fig. 4, the vertical resolution to determine the location of scattering is relatively poor. Since the required deviation of the propagation direction (scattering angle) is small, the scattering can happen almost anywhere between the source and receiver. However, it is known from array analysis of the $PKPdf$ precursor (Thomas et al., 1999, e.g.) that the most likely location of scattering is D". The theoretical possibility of propagating seismic energy in the time-distance window of the $PKPab$ precursor by $P*P$ scattering in the mid mantle (c.f. Fig. 4) is challenging to test because of the much stronger PKP phases. However, for scattering deeper in the mantle, the $P*P$ scattered waves can arrive prior to any scattered core phase and could be used to investigate scattering above D".

6 Conclusion

We show that the frequency range for investigation of the deep Earth with teleseismic waves can be extended towards frequencies of several Hertz. The attenuation of high frequency waves in the inner core allows for the observation of scattered $PKPbc$ waves as $PKPab$ precursor in the shadow of the inner core. Without this attenuation, the $PKPab$ precursor would be masked by the $PKPdf$ coda. This situation is similar to the $PKPdf$ precursor that can only be observed so clearly as the first arriving phase because the low velocity core deviates the P phase – thereby creating the (outer) core shadow.

We calculate the sensitivity kernels of the $PKPab$ precursor for heterogeneity using elastic radiative transfer simulations. The kernels describe the Earth's region in which scattering would contribute to seismic energys arrival in a given time-distance window. Scattering in D" that causes the $PKPdf$ precursor at $\Delta < 145°$ is also the most likely mechanism causing the $PKPab$ precursor at $\Delta > 155°$. Combining these sensitivities kernels with observations of scattered energy from $PKPab$ and $PKPdf$ precursors will improve the imaging and characterization of heterogeneity in the deep Earth .

Acknowledgments

K.B. acknowledges support from DAAD for his stay in Potsdam. Data from Japan (NIED, 2019), was kindly provided by the National Research Institute for Earth Science and Disaster Resilience and is available at www.hinet.bosai.go.jp. Data from Brazil was kindly provided by the Brazilian seismographic network (RSBR) and the participating institutions. It is available from www.rsbr.gov.br with details about access given in Bianchi et al. (2018).

References

Adam, J.-C., & Romanowicz, B. (2015). Global scale observations of scattered energy near the inner-core boundary: Seismic constraints on the base of the outer-core. *Phys. Earth Planet. Inter.*, *245*, 103–116. doi: 10.1016/j.pepi.2015.06.005

Bataille, K., & Lund, F. (1996). Strong scattering of short-period seismic waves by the core-mantle boundary and the P-diffracted wave. *Geophys. Res. Lett.*, *23*(18), 2413–2416. doi: 10.1029/96GL02225

Bianchi, M. B., Assumpção, M., Rocha, M. P., Carvalho, J. M., Azevedo, P. A., Fontes, S. L., ... Costa, I. S. (2018). The Brazilian seismographic network (RSBR): Improving seismic monitoring in Brazil. *Seismol. Res. Lett.*, *89*(2A), 452–457. doi: 10.1785/0220170227

Buffett, B. A., Garnero, E. J., & Jeanloz, R. (2000). Sediments at the top of earth's core. *Science (80-.).*, *290*(5495), 1338–1342. doi: 10.1126/science.290.5495.1338

Chang, A., & Cleary, J. (1978). Precursors to PKKP. *Bull. Seismol. Soc. Am.*, *68*(4), 1059–1079. doi: 10.1017/CBO9781107415324.004

Chang, A. C., & Cleary, J. R. (1981). Scattered PKKP: Further evidence for scattering at a rough core-mantle boundary. *Phys. Earth Planet. Inter.*, *24*(1), 15–29.

doi: 10.1016/0031-9201(81)90075-3
Courtillot, V. E., & Renne, P. R. (2003). On the ages of flood basalt events. *Comptes Rendus - Geosci.*, *335*(1), 113–140. doi: 10.1016/S1631-0713(03)00006-3
Earle, P., & Shearer, P. (2001). Distribution of fine-scale mantle heterogeneity from observations of Pdiff coda. *Bull. Seismol. Soc. Am.*, *91*(6), 1875–1881.
Earle, P. S., & Shearer, P. M. (1997). Observations of PKKP precursors used to estimate small-scale topography on the core-mantle boundary. *Science (80-.).*, *277*(5326), 667–670. doi: 10.1126/science.277.5326.667
Euler, G. G., & Wysession, M. E. (2017). Geographic variations in lowermost mantle structure from the ray parameters and decay constants of core-diffracted waves. *J. Geophys. Res. Solid Earth*, *122*(7), 5369–5394. doi: 10.1002/2017JB013930
Frost, D. A., & Rost, S. (2014). The P-wave boundary of the Large-Low Shear Velocity Province beneath the Pacific. *Earth Planet. Sci. Lett.*, *403*, 380–392. doi: 10.1016/j.epsl.2014.06.046
Gaebler, P. J., Sens-Schönfelder, C., & Korn, M. (2015). The influence of crustal scattering on translational and rotational motions in regional and teleseismic coda waves. *Geophys. J. Int.*, *201*, 355–371. doi: 10.1093/gji/ggv006
Gassner, A., Thomas, C., Krüger, F., & Weber, M. (2015). Probing the coremantle boundary beneath Europe and Western Eurasia: A detailed study using PcP. *Phys. Earth Planet. Inter.*, *246*, 9–24. doi: 10.1016/j.pepi.2015.06.007
Haddon, R. A. W., & Cleary, J. R. (1974). Evidence for scattering of seismic PKP waves near the mantle-core boundary. *Phys. Earth Planet. Inter.*, *8*(3), 211–234. doi: 10.1016/0031-9201(74)90088-0
Hansen, S. E., Carson, S. E., Garnero, E. J., Rost, S., & Yu, S. (2020). Investigating ultra-low velocity zones in the southern hemisphere using an Antarctic dataset. *Earth Planet. Sci. Lett.*, *536*, 116142. doi: 10.1016/j.epsl.2020.116142
Hedlin, M. A. H., Shearer, P. M., & Earle, P. S. (1997). Seismic evidence for small-scale heterogeneity throughout the Earth's mantle. *Nature*, *387*(6629), 145–150. doi: 10.1038/387145a0
Kennett, B. L., Engdahl, E. R., & Buland, R. (1995). Constraints on seismic velocities in the Earth from traveltimes. *Geophys. J. Int.*, *122*(1), 108–124. doi: 10.1111/j.1365-246X.1995.tb03540.x
Koelemeijer, P., Ritsema, J., Deuss, A., & van Heijst, H. J. (2016). SP12RTS: A degree-12 model of shear- and compressional-wave velocity for Earth's mantle. *Geophys. J. Int.*, *204*(2), 1024–1039. doi: 10.1093/gji/ggv481
Kustowski, B., Ekström, G., & Dziewoński, A. M. (2008). Anisotropic shear-wave velocity structure of the earth's mantle: A global model. *J. Geophys. Res. Solid Earth*, *113*(6), 1–23. doi: 10.1029/2007JB005169
Labrosse, S. (2014). Thermal evolution of the core with a high thermal conductivity. *Phys. Earth Planet. Inter.*, *247*, 36–55. doi: 10.1016/j.pepi.2015.02.002
Lay, T., & Garnero, E. J. (2011). Deep Mantle Seismic Modeling and Imaging. *Annu. Rev. Earth Planet. Sci.*, *39*(1), 91–123. doi: 10.1146/annurev-earth-040610-133354
Li, M., McNamara, A. K., & Garnero, E. J. (2014). Chemical complexity of hotspots caused by cycling oceanic crust through mantle reservoirs. *Nat. Geosci.*, *7*(5), 366–370. doi: 10.1038/ngeo2120
Margerin, L., Planès, T., Mayor, J., & Calvet, M. (2016). Sensitivity kernels for coda-wave interferometry and scattering tomography: theory and numerical evaluation in two-dimensional anisotropically scattering media. *Geophys. J. Int.*, *204*(1), 650–666. doi: 10.1093/gji/ggv470
McNamara, A. K. (2019). A review of large low shear velocity provinces and ultra low velocity zones. *Tectonophysics*, *760*(April 2018), 199–220. doi: 10.1016/j.tecto.2018.04.015

Monnereau, M., Calvet, M., Margerin, L., & Souriau, A. (2010, may). Lopsided growth of Earth's inner core. *Science*, *328*(5981), 1014–7. doi: 10.1126/science.1186212

Montagner, J. P., & Kennett, B. L. (1996). How to reconcile body-wave and normal-mode reference earth models. *Geophys. J. Int.*, *125*(1), 229–248. doi: 10.1111/j.1365-246X.1996.tb06548.x

Nakanishi, I. (1990). Highfrequency waves following PKPCDIFF at distances greater than 155°. *Geophy. Res. Lett*, *17*(5), 639–642.

NIED. (2019). *NIED Hi-net.* National Research Institute for Earth Science and Disaster Resilience. doi: 10.17598/NIED.0003

Obara, K., Kasahara, K., Hori, S., & Okada, Y. (2005). A densely distributed high-sensitivity seismograph network in Japan: Hi-net by National Research Institute for Earth Science and Disaster Prevention. *Rev. Sci. Instrum.*, *76*(2005), 021301. doi: 10.1063/1.1854197

Obara, K., & Sato, H. (1995). Regional differences of random inhomogeneities around the volcanic front in the Kanto-Tokai area, Japan, revealed from the broadening of S wave seismogram envelopes. *J. Geophys. Res.*, *100*(94), 2103–2121. doi: 10.1029/94JB02644

Okada, Y., Kasahara, K., Hori, S., Obara, K., Sekiguchi, S., Fujiwara, H., & Yamamoto, A. (2004). Recent progress of seismic observation networks in Japan - Hi-net, F-net, K-net and KiK-net. *Earth Planets Sp.*, *56*(XV-XXVIII). doi: 10.1088/1742-6596/433/1/012039

Olson, P. (2016). Mantle control of the geodynamo: Consequences of top-down regulation. *Geochemistry, Geophys. Geosystems*, *17*(5), 1935–1956. doi: 10.1002/2016GC006334

O'Rourke, J. G., & Stevenson, D. J. (2016). Powering Earth's dynamo with magnesium precipitation from the core. *Nature*, *529*(7586), 387–389. doi: 10.1038/nature16495

Pacheco, C., & Snieder, R. (2005). Time-lapse travel time change of multiply scattered acoustic waves. *J. Acoust. Soc. Am.*, *118*(3), 1300. doi: 10.1121/1.2000827

Ritsema, J., Deuss, A., Van Heijst, H. J., & Woodhouse, J. H. (2011). S40RTS: A degree-40 shear-velocity model for the mantle from new Rayleigh wave dispersion, teleseismic traveltime and normal-mode splitting function measurements. *Geophys. J. Int.*, *184*(3), 1223–1236. doi: 10.1111/j.1365-246X.2010.04884.x

Sato, H., Fehler, M., & Maeda, T. (2012). *Seismic Wave Propagation and Scattering in the Heterogeneous Earth* (second ed.). Heidelberg: Springer.

Schuberth, B. S., Bunge, H. P., & Ritsema, J. (2009). Tomographic filtering of high-resolution mantle circulation models: Can seismic heterogeneity be explained by temperature alone? *Geochemistry, Geophys. Geosystems*, *10*(5). doi: 10.1029/2009GC002401

Sens-Schönfelder, C., Margerin, L., & Campillo, M. (2009, jul). Laterally heterogeneous scattering explains Lg blockage in the Pyrenees. *J. Geophys. Res.*, *114*(B7). doi: 10.1029/2008JB006107

Shearer, P. M. (2007). *Deep Earth Structure - Seismic Scattering in the Deep Earth* (Vol. 1). Elsevier B.V. doi: 10.1016/B978-044452748-6.00021-3

Shen, Z., Ni, S., Wu, W., & Sun, D. (2016). Short period ScP phase amplitude calculations for core-mantle boundary with intermediate scale topography. *Phys. Earth Planet. Inter.*, *253*, 64–73. doi: 10.1016/j.pepi.2016.02.002

Sun, D., Helmberger, D. V., Jackson, J. M., Clayton, R. W., & Bower, D. J. (2013). Rolling hills on the core-mantle boundary. *Earth Planet. Sci. Lett.*, *361*, 333–342. doi: 10.1016/j.epsl.2012.10.027

Tackley, P. J. (2012). Dynamics and evolution of the deep mantle resulting from thermal, chemical, phase and melting effects. *Earth-Science Rev.*, *110*(1-4), 1–25. doi: 10.1016/j.earscirev.2011.10.001

Takeuchi, N. (2016). Differential Monte Carlo method for computing seismogram envelopes and their partial derivatives. *J. Geophys. Res. Solid Earth*, *121*(5), 3428–3444. doi: 10.1002/2015JB012661

Tanaka, S. (2005). Characteristics of PKP-Cdiff coda revealed by small-aperture seismic arrays: Implications for the study of the inner core boundary. *Phys. Earth Planet. Inter.*, *153*(1-3), 49–60. doi: 10.1016/j.pepi.2005.05.007

Thomas, C., Weber, M., Wicks, C. W., & Scherbaum, F. (1999). Small scatterers in the lower mantle observed at German broadband arrays. *J. Geophys. Res. Solid Earth*, *104*(B7), 15073—-15088.

Trabant, C., Hutko, A. R., Bahavar, M., Karstens, R., Ahern, T., & Aster, R. (2012, 09). Data Products at the IRIS DMC: Stepping Stones for Research and Other Applications. *Seismological Research Letters*, *83*(5), 846-854. doi: 10.1785/0220120032

Wang, Y., & Wen, L. (2004). Mapping the geometry and geographic distribution of a very low velocity province at the base of the Earth's mantle. *J. Geophys. Res. Solid Earth*, *109*(10), 1–18. doi: 10.1029/2003JB002674

Wu, W., Ni, S., & Shen, Z. (2014). Constraining the short scale core-mantle boundary topography beneath Kenai Peninsula (Alaska) with amplitudes of core-reflected PcP wave. *Phys. Earth Planet. Inter.*, *236*, 60–68. doi: 10.1016/j.pepi.2014.09.001

Yu, S., & Garnero, E. J. (2018). Ultralow Velocity Zone Locations: A Global Assessment. *Geochemistry, Geophys. Geosystems*, *19*(2), 396–414. doi: 10.1002/2017GC007281

Zhang, S., Wang, R., Dahm, T., Zhou, S., & Heimann, S. (2020). Prompt elasto-gravity signals (PEGS) and their potential use in modern seismology. *Earth Planet. Sci. Lett.*, *536*, 116150. doi: 10.1016/j.epsl.2020.116150

Supporting Information for "High Frequency (6 Hz) PKPab precursors and their sensitivity to deep Earth heterogeneity"

C. Sens-Schönfelder[1], K. Bataille[2,1], M. Bianchi[3]

[1]GFZ German Research Centre for Geosciences, Telegrafenberg, 14473 Potsdam, Germany

[2]Earth Sciences Department, University of Concepcin, Chile

[3]Instituto de Astronomia, Geofsica e Cincias Atmosfricas, Universidade de So Paulo, Brazil

Contents of this file

Introduction In the following we describe the numerical simulations of the deep Earth scattering and of the data processing used to extract the signals of the $PKPab$ precursor. We also show the stacked envelopes of the HiNet records for each 1° distance bin.

Text S1. Differential Monte-Carlo Simulation of Deep Earth Scattering

Radiative Transfer Theory can describe the propagation of scattered seismic waves. We use a version of the elastic simulation code described by Sens-Schönfelder, Margerin, and Campillo (2009) that we adapted to spherical geometry with a 1D velocity and attenuation structure. This code has already been used to model the teleseismic waves by Gaebler, Sens-Schönfelder, and Korn (2015). To highlight the effects of localized scattering, we introduce a further conceptual modification that allows us to directly model the *change* of seismic intensity due to the presence of scattering in a specified part of the model. We call this differential modeling. Takeuchi (2016) has used a similar approach.

In the Radiative Transfer approach, the propagation of seismic wave energy is simulated by the number density of a large number of particles (wave packets). The particles propagate through the domain according to the ray theory. Scattering is simulated by discrete scattering events governed by the statistical properties of the medium's heterogeneity. Intrinsic attenuation is accounted for by reducing the weight of the particles.

To simulate the differential intensity, we modify the weights of the particles by an additional factor (S). Let us call the region under investigation G in which the change in scattering properties should be modeled. When particles are launched from the source we set $S = 0$. This changes only upon scattering in G. When a particle is scattered in G we have to model the increase of scattered intensity as well as the decrease of ballistic intensity. This is done in a probabilistic sense by either changing the direction of the particle and setting $S = 1$ to simulate the increase of scattered intensity with a probability of 50% or by simply setting $S = -1$ and keeping the propagation direction to simulate the decrease of ballistic intensity with a probability of 50%. A particle with $S = -1$ does not interact with the heterogeneity in the G.

The simulations in this paper use a modified version of the ak135-f model (Kennett et al., 1995; Montagner & Kennett, 1996) obtained from the IRIS DMC Data products (Trabant et al., 2012) with doi:10.17611/DP/9991801. The modification comprised replacing the shallow partly liquid structure at the Earths surface with constant structure corresponding to the top side of the discontinuity at 10 km depth.

Text S2. Processing of Envelope Stacks

The high frequency seismograms that we use to observe the scattered wave are affected by local noise, site factors and station sensitivity. To visualize the stacked envelopes, we use the following processing steps.

1. data selection
2. filtering
3. envelope calculation using instantaneous amplitude
4. temporal smoothing of logarithmic envelopes
5. alignment to reference phase travel time
6. stacking of logarithmic envelopes in distance bins
7. subtraction of noise level
8. normalization to the maximum amplitude value

Figure S1. Data of the $PKPab$ precursor

Here we show the data used to create the color images of the time-distance sections as individual traces, with gray background indicating the pointwise logarithmic standard deviation when different records have been stacked. Figures S1 and S2 show the data from the Jan 1st 2011 Argentina event recorded by the HiNet stations in Japan, processed as described above but without the normalization to the maximum in the last item.

References

Gaebler, P. J., Sens-Schönfelder, C., & Korn, M. (2015). The influence of crustal scattering on translational and rotational motions in regional and teleseismic coda waves. *Geophys. J. Int.*, *201*, 355–371. doi: 10.1093/gji/ggv006

Kennett, B. L., Engdahl, E. R., & Buland, R. (1995). Constraints on seismic velocities in the Earth from traveltimes. *Geophys. J. Int.*, *122*(1), 108–124. doi: 10.1111/j.1365-246X.1995.tb03540.x

Montagner, J. P., & Kennett, B. L. (1996). How to reconcile body-wave and normal-mode reference earth models. *Geophys. J. Int.*, *125*(1), 229–248. doi: 10.1111/j.1365-246X.1996.tb06548.x

Sens-Schönfelder, C., Margerin, L., & Campillo, M. (2009, jul). Laterally heterogeneous scattering explains Lg blockage in the Pyrenees. *J. Geophys. Res.*, *114*(B7). doi: 10.1029/2008JB006107

Takeuchi, N. (2016). Differential Monte Carlo method for computing seismogram envelopes and their partial derivatives. *J. Geophys. Res. Solid Earth*, *121*(5), 3428–3444. doi: 10.1002/2015JB012661

Trabant, C., Hutko, A. R., Bahavar, M., Karstens, R., Ahern, T., & Aster, R. (2012, 09). Data Products at the IRIS DMC: Stepping Stones for Research and Other Applications. *Seismological Research Letters*, *83*(5), 846-854. doi: 10.1785/0220120032

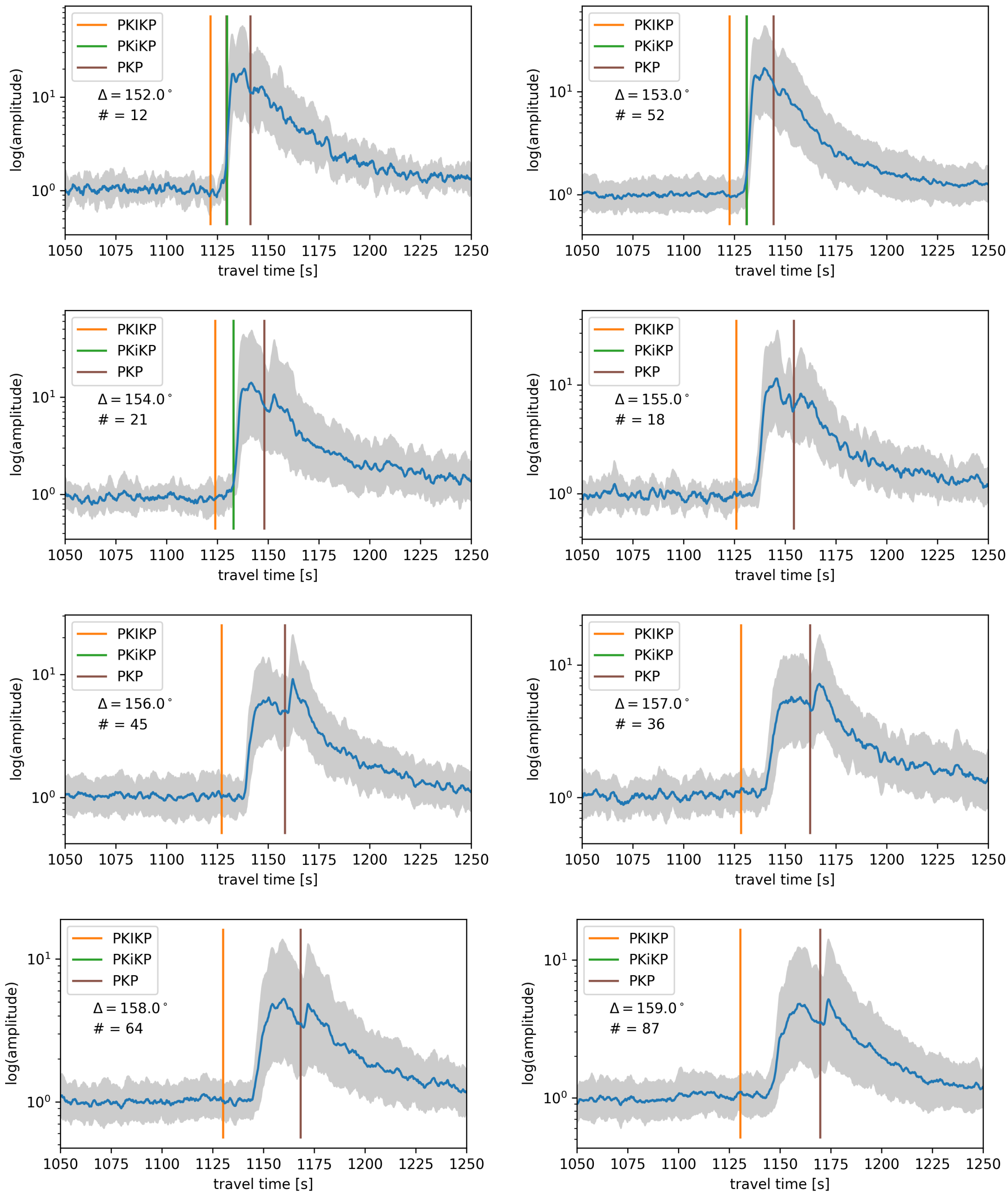

Figure S1. Stacked HiNet records of the Jan 1st 2011 Argentina event for 1° wide bins cantered at the distances given in each panel. The number of stacked records is indicated in each panel.

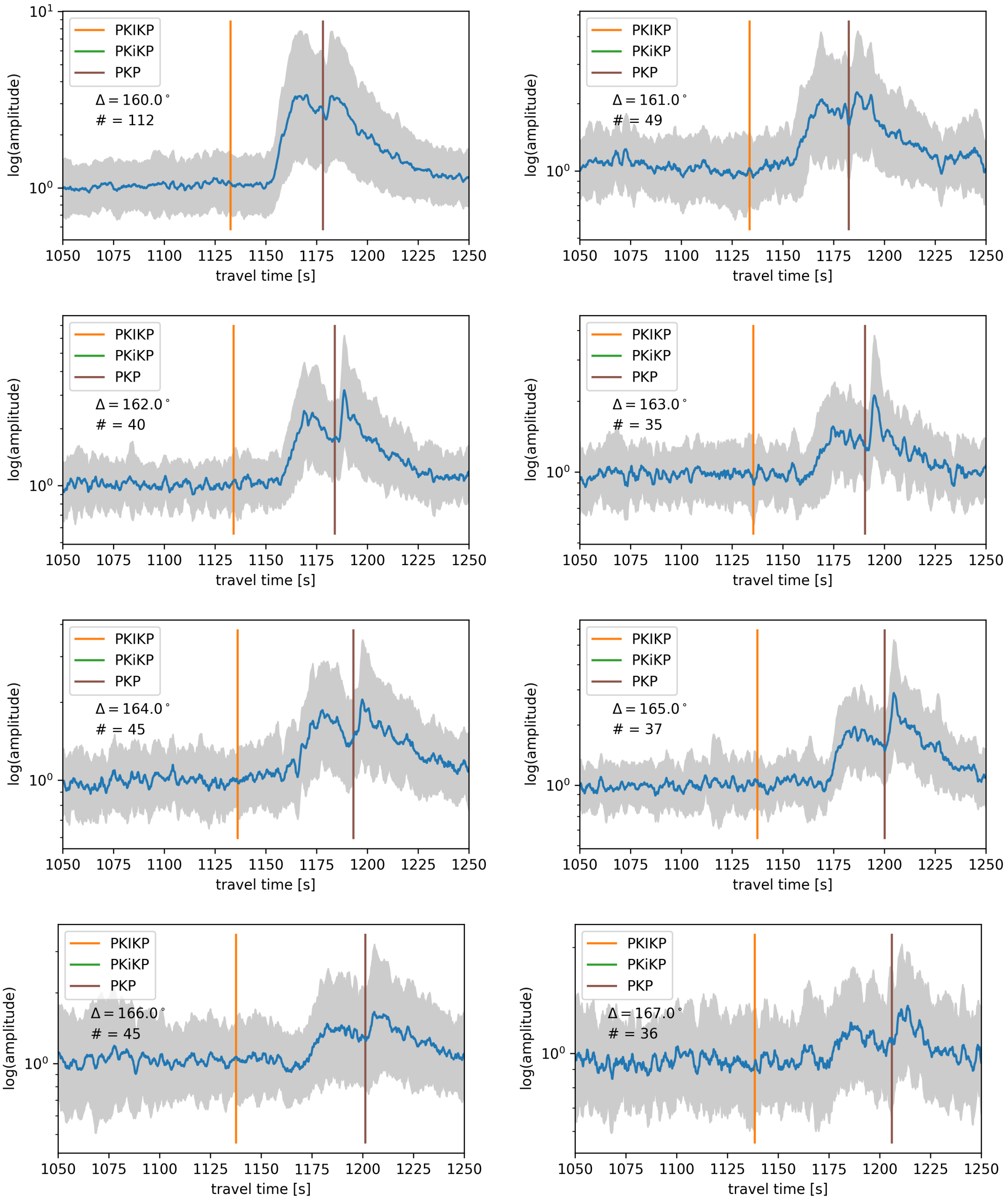

Figure S2. Same as Fig. S1 for further distances.